

Local alkali-metal-promoted oxidation of Si(100)-(2×1) surfaces: A generalized-Hubbard-model calculation

M. C. Refolio, J. M. López Sancho, M. P. López Sancho, and J. Rubio

Instituto de Ciencia de Materiales de Madrid, Consejo Superior de Investigaciones Científicas, Serrano 144, 28006 Madrid, Spain

(Received 2 August 1993)

In order to study the local regime in the alkali-metal-promoted oxidation of silicon, we consider the coadsorption of an oxygen molecule and a potassium atom on the dimerized Si(100)-(2×1) surface. Antiferromagnetic (singlet) spin correlations within the Si dimers are taken into account from the outset by working with a generalized Hubbard Hamiltonian. In this background, the adsorption of a K atom strongly polarizes the medium creating a local charge-spin bag, around the K^+ ion, which sets the scenario for promoted oxidation. When an O_2 molecule in its ground state ($^3\Sigma_g^-$) approaches this region of the surface, it is influenced by the attractive electrostatic field of the K^+ ion, with the corresponding lowering of its affinity level. This eventually crosses the Fermi level and captures the excess electron charge in the bag. A superoxide O_2^- ion, the $^2\Pi_g$ state, is thereby formed, ionically bonded to K^+ and covalently bonded to the Si dimer. In the absence of potassium, the oxygen molecule simply physisorbs in a state adiabatically connected to its gas-phase ground state.

I. INTRODUCTION

The formation of abrupt, atomically perfect Si-SiO₂ interfaces is very important in silicon-derived technology. But direct oxidation of a bare Si orbital requires high temperature and elevated pressures to speed the reactions,¹ which in turn cause changes in the electronic characteristics of the devices by dopants diffusion and structural modification. Therefore, great interest has been devoted to the enhancement, by many orders of magnitude, of Si oxidation produced by the presence of preadsorbed noble, transition, rare-earth²⁻⁸ and alkali metals.⁹⁻¹⁷ Problems of interdiffusion and chemical reaction between adatoms and silicon appear in all metals except Na, K, and Cs, which can be desorbed, after SiO₂ formation, by heating to moderate temperature.

In addition, the alkali-metal-promoted oxidation of Si, due to the lack of interdiffusion of both elements, is a well-defined system in studying fundamental mechanisms of catalytic processes. The role of the alkali metals in promoting oxidation reactions is, however, a matter of controversy in experimental and theoretical studies. The essential steps taking place in the Si oxidation are,¹⁸ therefore, as follows: (a) trapping of the incoming oxygen molecule, (b) transition of the adsorbed O_2 into an excited state, this process being the rate-controlling step, (c) transfer of Si dangling-bond charge to the adsorbed molecule, leading to dissociation, and (d) chemical bonding of the O atoms to the Si substrate. Based on this scheme, several mechanisms have been proposed which can be classified into two categories regarding the local or nonlocal nature of the microscopic process. The relationship between the resulting amount of oxide, for a given oxygen exposure, and the alkali-metal coverage should be a rigorously linear function if produced by a local mechanism. Therefore, any deviation from proportionality at low coverage would point to nonlocal activation processes.

It seems by now clear that oxygen adsorption is non-dissociative in nature, even in transition metals. Consequently O_2 must undergo a transition to an O_2^- configuration first stable on the surface, but then dissociated due to charge transfer from that surface. Oxygen detected on the surface is only associated with KO₂ and SiO₂ molecules after high dosages of oxygen. Based on this fact, Ernst and Yu¹⁹ measured the absolute value of the O_2 initial sticking coefficient versus Cs coverage, instead of the maximum amount of oxide formed after oxygen saturation. Similar results were found by other groups using x-ray photoemission spectroscopy,^{10-12,20} also detecting the oxygen of SiO₂ and KO.

Miranda and co-workers,¹⁰⁻¹² using Auger-electron spectroscopy and photoemission of adsorbed xenon,²⁰ reported a linear relationship between the alkali-metal coverage and the amount of SiO₂ formed, thus supporting the local catalytic picture. In contrast, Soukiassian and co-workers,¹³⁻¹⁸ using photoemission spectroscopy, observed a nonlinear relationship between SiO₂ formation and alkali adsorption (with a threshold coverage of about 0.5 monolayer) concluding that the catalytic effect is non-local in nature.

The theoretical models are also equally divided, although they all agree in that the dissociation of O_2 is the rate-determining step of the oxidation process. Norskov, Holloway, and Lang²¹ suggested that the local electric dipole of the alkali substrate complex increases the molecular adsorption energy, lowering the antibonding $2\pi^*O_2$ level. The filling of this level produces then oxygen dissociation. Hellsing²² postulates a $^3\Sigma_g^- \rightarrow ^1\Delta_g$ transition in the oxidation of silicon, whereas Panas and co-workers²³ proposed a $^3\Sigma_g^- \rightarrow ^3\Delta_u$ transition in the oxidation of Ni(100).

As to the Si(100)-(2×1) surface, cluster calculations reveal that spin correlations can be important for this surface. In calculations by Artacho and Yndurain,²⁴ which consider the effect of on-site interactions in symmetric

and asymmetric dimer models, it is found that an antiferromagnetic (AF) spin arrangement within the dimers lowers the total energy and opens an AF gap in the surface band structure. The surface is then always semiconducting, irrespective of the dimer model, while the AF energy lowering (> 1 eV/dimer) strongly outweighs any energy differences between different geometric models. Thus, whatever the dimer model adopted, spin correlations seem essential to explain the electronic structure of this surface. It should be noted that these AF spin correlations quickly drop to zero outside the dimers for the moderate U values appropriate to this surface, so that no long-range AF spin order actually occurs. Only the spin-singlet arrangement within the dimers survives.

In the present work we adopt this AF description of the clean surface, as in previous work,²⁵ but now we explore its consequences in an attempt to attain a comprehensive understanding of the local promotion effect (adsorption of a single K) on the oxidation of the Si(100)-(2×1) surface. A detailed application of the present model will be made to the oxidation of both clean and alkali locally covered Si(100)-(2×1) surfaces along the two reaction paths proposed by Hellsing²² and Panas and coworkers.²³

The calculations are performed for an array of 300 Si atoms forming three rows of 50 dimers with periodic boundary conditions (PBC). To study the local O₂-K interaction, we will adsorb a single alkali atom on the valley-cave site, between two dimer rows, followed by the oxygen molecule in a pedestal-bridge position, over a Si dimer (Fig. 1). For a discussion of the adsorption sites, see Michel *et al.*²⁶ Since the adsorbed potassium atom is in an ionized state, its attractive Coulomb interaction with the first-neighbor Si atoms lowers locally the corresponding Si density of states (DOS). The upper, initially unoccupied, Si Hubbard band then crosses the Fermi level. The local adsorption of O₂ at this site can therefore be rather similar to oxygen adsorption on a metal.

II. MODEL AND HAMILTONIAN

We start out with a Hamiltonian of the type

$$H = H_{\text{Si}} + H_{\text{O}_2} + H_{\text{K}} + H' \quad (1)$$

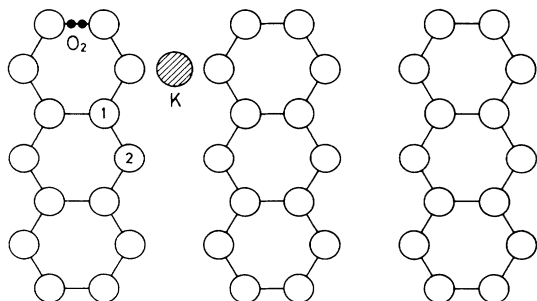


FIG. 1. Diagram of adsorption sites for the potassium-promoted oxidation of Si(100)-(2×1) surfaces. Small black circles: O₂ molecule on dimer-bridge site. Shaded circle: K on valley-cave site. White circles denote silicon atoms. The first layer (1) contains the dimers. For perspective, the second layer (2), formed by an ideal $\langle 110 \rangle$ plane, is also shown.

indicating schematically three subsystems, the silicon surface, the oxygen molecule, and a single potassium atom, in mutual interaction. The detailed form of this Hamiltonian will be now given in conjunction with the specific model adopted for the different situations.

A. The substrate (a Si surface)

We take the reconstructed Si(100)-(2×1) surface as a collection of symmetric dimers forming three rows of 50 dimers along the $\langle 110 \rangle$ direction. The intradimer distance is 2.24 Å, the dimers being spaced along the rows by 3.84 Å, while the distance between rows (equivalent points) is 7.68 Å. No consensus has been reached about the buckled or unbuckled nature of the dimers. The calculations always give energies too close in both cases to resolve ambiguities. Recently, Wolkow²⁷ has obtained remarkable results by observing this surface at different temperatures, concluding that the buckled-surface geometry has the lowest energy. But both forms are so close that Si(100) always shows rows of buckled dimers even at room temperature. Pairs of adjacent dimers with anticorrelated tipping angles as well as unbuckled dimers have also been observed, leading to an image of the surface with both buckled and unbuckled dimers in a comparable amount. (For a discussion, see Stillinger²⁸.) Therefore, we adopt in this work a model of symmetric unbuckled dimers. We want to stress at the outset, however, that the exact geometry and nature of the dimers (buckled or not) have only a minor effect on the magnetic spin distribution, strongly dominated by the Hubbard on-site repulsions. These will be shown to play a role in both the adsorption of electropositive atoms and the electronic transitions we consider in this paper.

There are four surface dangling-bond bands: Two of them are of σ symmetry (one formed by σ -bonding molecular levels, well below the bulk band gap, and the other formed by the empty σ^* -antibonding levels, far above this gap). They will play no role in what follows. The other two bands are of π symmetry (π and π^*), lying just in the gap region and being populated by two electrons per Si dimer (or one electron per Si atom). These π bands will be considered in what follows as arising from a half-filled Hubbard band^{24,25} with an AF insulating gap of the Mott-Hubbard type. Therefore, we describe the Si surface by the Hubbard Hamiltonian

$$H_{\text{Si}} = E_{\text{Si}} \sum_{is} n_{is} + \sum_{\langle ij \rangle_s} t_{ij} c_{is}^{\dagger} c_{js} + U_{\text{Si}} \sum_i n_{i\uparrow} n_{i\downarrow}, \quad (2)$$

where the indices i and j run through all the Si atoms with the restriction, suggested by the symbol $\langle \rangle$ in the double sum, that only first- and second-order neighbors are connected by hopping (t_{ij}). U_{Si} denotes the one-center Coulomb repulsion on the Si atoms, one of the main ingredients of this model. A weak interchain coupling has been allowed so as to always have a two-dimensional system. Finally, PBC are used along both planar axes in order to keep size effects to a minimum. The t_{ij} parameters (intradimer hopping, as well as first- and second-order band hopping) are scaled with Harrison's²⁹ rules which leave just a single t . This, along

with E_{Si} and U_{Si} , fix the overall width of the band structure, the Fermi level (-4.5 eV), and gap (0.6 eV), respectively. The intra-atomic repulsion turns out to be $U_{\text{Si}} = 1$ eV.²⁵ The silicon DOS for both spins are given in Fig. 2.

B. The adsorbate (an oxygen molecule)

The O_2 molecule is characterized by the three $2p$ -derived levels corresponding to the π_z bonding and the π_x^* and π_y^* antibonding orbitals, when considering as frozen the rest of the orbitals during the adsorption process. In this picture the yx plane is parallel, while the yz plane is perpendicular to the surface, as shown in Fig. 3. The adsorption bond is formed through the interaction of the π_z and π_x^* orbitals of the O_2 molecule with the two dangling bonds (opposite spins) of the dimer. The π_x^* orbital is normal to the Si dangling bonds. We thus write the Hamiltonian

$$H_{\text{O}_2} = \sum_{ab} E_a n_{as} + \frac{1}{2} \sum_{as \neq bs'} (U_{ab} - J_{ab} \delta_{ss'}) n_{as} n_{bs'}, \quad (3)$$

where the summations run over the three orbitals participating in the adsorption bond of energy E_a and connected by Coulomb (U) and exchange (J) integrals. These are adjusted to give, in the gas phase, the ionization as well as the first and second affinity potentials of the O_2 molecule in its ground state. They are $I = 12.07$ eV, $A_1 = 0.44$ eV, and $A_2 = -5.9$ eV according to the calculation of Goddard III, Redondo, and MacGill.³⁰ These three levels play an important role in the adsorption and promo-

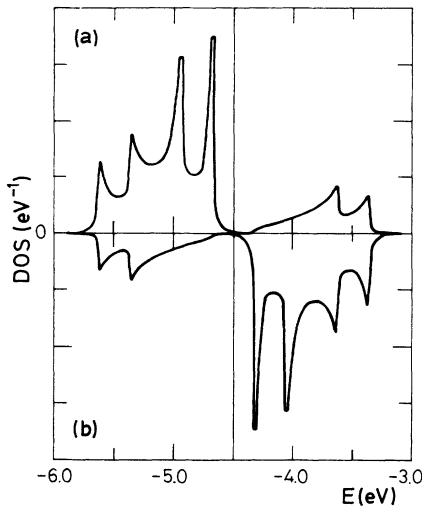


FIG. 2. Spin-polarized density of states (DOS) projected on an atom of the reconstructed $\text{Si}(100)-(2 \times 1)$ surface, showing the Fermi level (thin vertical line) at the midpoint of the gap. (a) majority spin; (b) minority spin. Energies are referred to the vacuum level. The calculation has been done for a cluster of 50×3 dimers with periodic boundary conditions. A Lorentzian broadening has been used with full width at half maximum equal to the mean separation between the cluster single-particle levels.

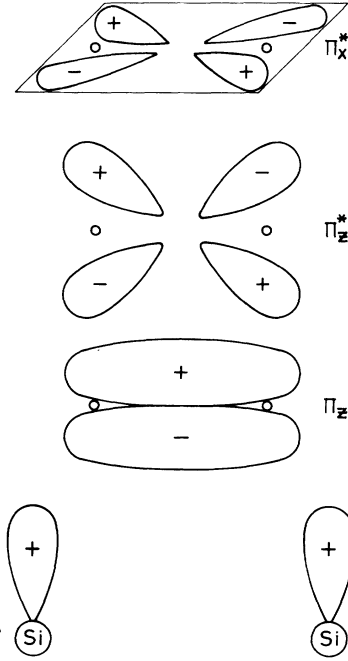


FIG. 3. Diagram of the free dangling bonds of a $\text{Si}(100)-(2 \times 1)$ dimer (bottom) as well as relevant oxygen molecular orbitals in the adsorption process.

tion process to be described subsequently. The adjustment is made through a second-degree polynomial in the molecular charge.

C. The promoter (an alkali atom: potassium)

The potassium atom is here characterized by a single-level atom, i.e.,

$$H_K = E_K \sum_s n_{Ks} \quad (4)$$

with the level $E_K = -2.7$ eV. Since the final potassium charge will be very small, no intra-atomic Hubbard U need to be considered on the potassium atom.

D. Switching on the interactions

The three subsystems are now coupled by hopping and Coulomb integrals

$$H' = \sum_{\langle \alpha\beta \rangle s} V_{\alpha\beta} c_{\alpha s}^{\dagger} c_{\beta s} + \frac{1}{2} \sum_{\langle \alpha\beta \rangle} U_{\alpha\beta} (n_{\alpha} - n_{\alpha}^0)(n_{\beta} - n_{\beta}^0), \quad (5)$$

where α, β now run over the silicon, oxygen, and potassium orbitals. Since we will be faced with large charge transfers, the Coulomb interaction between them is essential. The notation is $n_{\alpha} = n_{\alpha\uparrow} + n_{\alpha\downarrow}$ and n_{α}^0 means the initial occupation of the α th level. The two-center Coulomb integrals will be approximated by the expression of Mataga and Nishimoto³¹ in the form given by Ramaker³² for SiO_2 :

$$U_{\alpha\beta} = e^2 [R_{\alpha\beta} + 2e^2 / (U_\alpha + U_\beta)]^{-1}, \quad (6)$$

where U_α is the Hubbard intra-atomic repulsion of the α th orbital and $R_{\alpha\beta}$ is the internuclear distance. This approximation takes an average between two extreme situations: for large distances $U_{\alpha\beta} = e^2 / R_{\alpha\beta}$ and for small distances $U_{\alpha\beta} = (U_\alpha + U_\beta) / 2$. The mixing hopping integrals, however, are more tricky. Although they will be scaled with distance by Harrison rules,²⁹ three free parameters still survive, $V_{\text{Si-K}}$, $V_{\text{Si-O}}$, and $V_{\text{O-K}}$. We take $V_{\text{Si-O}}$ from Harrison's adjustment for the SiO_2 compound at the equilibrium distance, 1.61 Å (Ref. 29, pp. 261–273). The other two parameters follow very simply from the geometric mean rule,²⁹ the already adjusted t_{Si} , and a representative potassium hopping integral, t_{K} (4.52 Å) = 0.25 eV fitted to obtain just the lowest s band of the bulk K band structure. An image potential, $V_{\text{im}} = 1 / (4d)$ (d being the O_2 -Si distance), is also included with the corresponding modification of the energy levels and Coulomb integrals of the adsorbate. Similar comments apply to the promoter.

We want to stress at this point that our extensive use of scaling laws with distance, the geometric mean rule for mixing hopping integrals, and prescription (6) for interatomic Coulomb integrals strongly reduces the number of parameters and renders a virtually parameter-free model. Indeed, the few parameters thereby left are fixed by the dangling-bond band structure of silicon as well as by the ionization and affinity levels of both adsorbate and promoter.

The Hamiltonian just described is now decoupled in a self-consistent field unrestricted Hartree-Fock (UHF) approximation where both the charge and spin (transverse and longitudinal) components on the Si atoms are considered on the same footing. The two-center Coulomb terms are linearized in a simple Hartree-Fock approximation.²⁵

III. ACTIVATED VERSUS PROMOTED DISSOCIATION PROCESSES

The linearized Hamiltonian just described is now diagonalized for the following situations: (1) The O_2 molecule placed at a pedestal bridge on the clean Si surface; (2) A single K atom on a valley-cave adsorption site, and (3) The O_2 molecule on a pedestal bridge near the preadsorbed K atom. These three cases are studied for different surface-adsorbate distances. We also consider the approaching molecule to be in different initial states in order to test the role of the transitions between them as possible rate-limiting steps in the dissociation reaction. The interactions described in the preceding section will now be, accordingly, switched on as needed. The initial charges on the oxygen levels will have to be likewise modified.

A. Isolated oxygen adsorption: climbing the hill

It is generally admitted that the dissociation of the O_2 adsorbed molecule takes place through a superoxide O_2^- state.^{22,23,33} This ionic state places charge into the π^* an-

tibonding O_2 molecular orbitals, thereby increasing their O-O distance. It is by now well known³³ that, in this configuration, the O_2 axis is parallel to the surface, the outermost oxygen orbitals interacting with the dangling bonds of two Si atoms. We therefore adsorb a single O_2 molecule in bridge position over a Si dimer and study its interaction, as a function of the oxygen-surface distance, for two different states of O_2 : the ground state (GS), the $^3\Sigma_g(\pi_{z\uparrow}\pi_{x\uparrow}\pi_{z\uparrow})$ triplet with the neutral surface, and the superoxide form $^2\Pi_g(\pi_{x\uparrow}\pi_{x\downarrow}\pi_{z\uparrow})$ with the Si surface ionized.

In Fig. 4, we represent the electron-energy curves of these configurations against distance to the surface. The lowest curve is that adiabatically derived from the oxygen GS. The arrows mark the estimated region where the minimum of the corresponding Born-Oppenheimer curve lies. Since, clearly, the O_2^- curve does not cross the GS adsorption curve before reaching the minimum, no direct transition can take place. The capture of one electron by the adsorbed oxygen molecule, therefore, requires some excitation process (i.e., activated process), as the one proposed by Helsing or Panas and co-workers.

According to Helsing,²² the excitation is to the $^1\Delta_g(\pi_{z\uparrow}\pi_{x\downarrow})$ singlet via the electronic transition $\pi_{z\uparrow}^* \rightarrow \pi_{x\downarrow}^*$. In the GS, the π_z^* orbital lies closest to the surface and repels the dangling-bond charge. The spin-flip transition empties the π_z^* molecular orbital, thus allowing its approach to the surface. At short enough distance, higher values of both image potential and hopping can lead to recapture of the electron by the π_z^* orbital with the formation of O_2^- , an activated process almost universally considered as the rate-controlling step for dissociation. In the mechanism proposed by Panas and co-workers²³ for the dissociation of oxygen on Ni(100), the excitation is to the $^3\Delta_u$ state ($\pi_{z\uparrow}\pi_{x\downarrow}\pi_{z\uparrow}$). This state is reached from the GS via a $\pi_{z\downarrow} \rightarrow \pi_{x\downarrow}^*$ transition which leaves O_2 in a situation similar to that of the Helsing process. The lowering of the repulsion energy between Si and O_2 is now due to the hole produced in the π_z , instead of in the π_z^* molecular orbital.

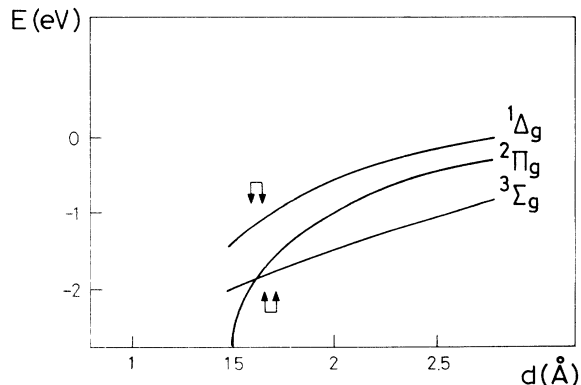


FIG. 4. Electron-energy curves against oxygen-surface distance for the ground state ($^3\Delta_g$), the superoxide ion ($^2\Pi_g$), and the excited singlet ($^1\Delta_g$) of the Helsing process. Arrows mark estimated distance where minimum of the corresponding Born-Oppenheimer curve occurs.

When the Si on-site repulsions are taken into account, however, these processes are subject to some restrictions displayed in Fig. 5. In Helsing's process, two elementary virtual steps are needed to achieve a spin-flip transition, e.g., one must have $\pi_{z\uparrow}^* \rightarrow \text{Si}_\uparrow$ followed by $\text{Si}_\downarrow \rightarrow \pi_{x\downarrow}^*$ [Fig. 5(a)], going through a doubly occupied Si dangling bond and ending up in a state with its AF order distorted (relaxed afterwards) by the presence of two neighbor up-spin Si atoms, thus leading to a net energy rise by $\sim U_{\text{Si}}$. In Fig. 5(b) we have represented schematically the alternative process of Panas and co-workers, which now requires the successive transitions $\pi_{z\downarrow} \rightarrow \text{Si}_\downarrow$ followed by $\text{Si}_\uparrow \rightarrow \pi_{x\uparrow}^*$. The final situation keeps now the AF order unchanged, thus lowering its energy by about 1 eV.

Figure 6 shows, finally, the energy-level diagram of the four $\text{O}_2 + \text{Si}$ configurations we are considering, before switching on the surface-adsorbate interactions. We can surmise that ${}^3\Delta_u$ lies about 2.2 eV higher than ${}^1\Delta_g$ and, therefore, the transition of Panas and co-workers is much less probable at low temperature than the Helsing transition. On the other hand, since the state ${}^3\Delta_u$ is not a long-lived one, it cannot lead to a new dissociation mechanism via a Coulomb explosion.³⁴ Turning then to the Helsing process, Fig. 4 also shows that the transition ${}^3\Sigma_g^- \rightarrow {}^1\Delta_g$ takes about 0.8 eV. Once on this curve, with the surface-adsorbate repulsion lowered, O_2 would

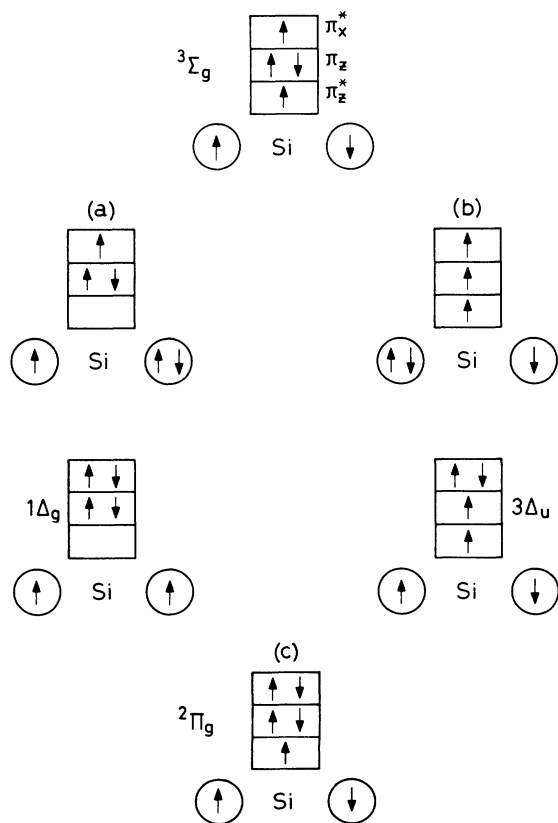


FIG. 5. Schematic diagram of the intermediate steps leading from the ground state of the oxygen molecule (top) to the formation of a superoxide ion (c) along the process proposed by (a) Helsing or (b) Panas and co-workers.

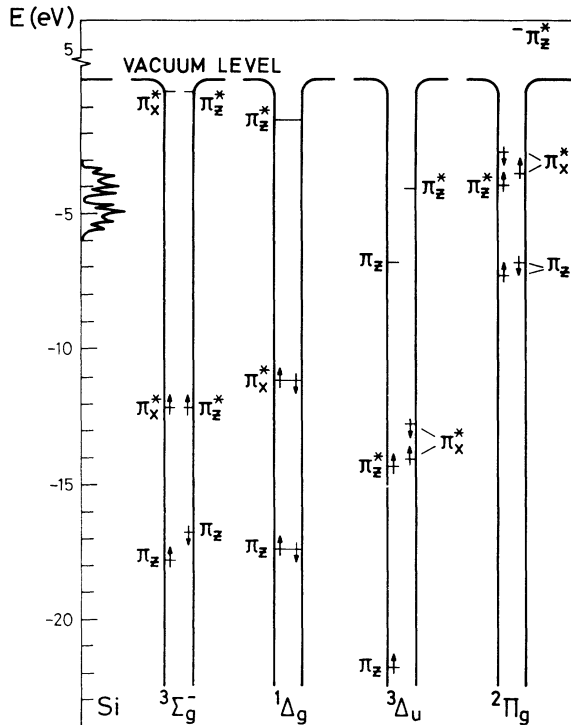


FIG. 6. Level diagram of the $\text{Si} + \text{O}_2$ configurations considered in this work at infinite separation, i.e., before switching on the interactions. Energies are referred to the vacuum level.

come closer to the Si surface. At about the O_2 equilibrium distance, the π_z^* level would cross the Fermi level and capture an electron from the surface, thereby forming an ionized species (bottom of Fig. 5). This excitation from the GS to the superoxide form of O_2 stretches the O-O distance, with a concomitant increase in the overlap of π_z^* with the dangling bonds of the Si dimers. This process leads to the dissociation of O_2 with an activation energy of ~ 0.8 eV.

B. Adsorption of the promoter: setting the local scenario

In order to study the local promotion effect, we place a single K atom on the $\text{Si}(100)-(2 \times 1)$ cluster. Direct measurement by Kendelewicz *et al.*³⁵ gives a potassium-silicon distance $d_{\text{Si-K}} = 3.14 \text{ \AA}$ and, after the work of Michel *et al.*,³⁶ we place the K atom in a cave interrow position (Fig. 1). It will be evident later that the enhancement of the dissociation is higher in this position than in any other interrow or on-top adsorption site.

Si on-site repulsions play an important role in the charge-transfer process from K to Si. This is because hopping mixes only electrons of the same spin and, thus, polarizes the AF Si surface, creating a spin-charge bag around the K^+ ion. But we must not forget the Coulomb attraction between Si and K^+ ($U_{\text{Si-K}} = 0.5$ eV) which enhances the localization of the Si charge near K^+ . This can be visualized as the formation of a shallow depression in the Si-projected DOS, due to the downshift of its levels by some 0.6 eV, in a region of about two unit cells around

the potassium atom. Almost 95% of the total transferred charge (0.93) is localized in this region.

Figure 7 displays the spin-charge bag around the potassium ion, showing both the distorted AF order and the distribution of the transferred charge surrounded by a dashed line. The distribution outside this line is just that of the clean surface. These results can be compared with the experimental ones obtained by Castro *et al.*²⁰ by photoemission of adsorbed xenon at low temperatures. These authors report a difference between the local field at clean Si(100) and in the neighborhood of the K adatom of 0.5 eV, which reflects the combined effect of the K^+ electrostatic field and the charge redistribution. They found this decrease in the surface potential to be localized within a distance of 4 Å, in good agreement with our results (Fig. 7).

We find an electronic contribution to the potassium chemisorption energy of 3.1 eV, which compares well with the experimental value of about 2.2 eV in the early stages of K adsorption³⁶ and with the 3 eV calculated by Ling, Freeman, and Delley.³⁷ These results imply a nuclear repulsion of some 0.8–1 eV, which is quite reasonable. We have not dealt with the local work function, but our results for the charge transfer and charge localization are in qualitative agreement with the consensus on the decrease of the Si work function up to a maximum of about 3 eV.

To summarize, our calculations show that the adsorption of a potassium atom modifies the Si(100)-(2×1) surface, forming a patch of limited extension (~ 2 unit cells)

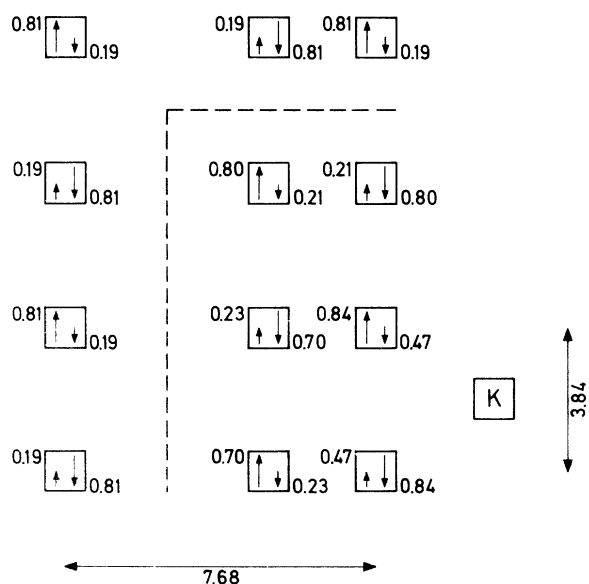


FIG. 7. Diagram of the charge-spin bag around an adsorbed potassium atom on a valley-cave site of the Si(100)-(2×1) surface. Squares with arrows denote Si atoms, the length and tip of the arrows referring to the up and down spins. Numbers on both sides of each square give the population with spin up and spin down. Since the bag is of fourthfold symmetry around the potassium atom, only the top-left quadrant has been shown. The dashed line surrounds the K-affected region, the distribution outside being that of the clean surface.

where the AF spin and charge distributions are distorted. Beyond this region, the surface is unperturbed. This is the local scenario for promoted oxygen adsorption.

C. Adsorbate and promoter together: opening the path to dissociation

Finally we adsorb the O_2 molecule on one of the pedestal bridges of this local scenario provided by the charge-spin bag surrounding K^+ . The Hamiltonian is now diagonalized for the three O_2 initial states described in Sec. III A. The electron-energy curves versus distance are given in Fig. 8, showing a general picture of the process significantly different from that of O_2 adsorption on the clean Si surface: First, the adsorption energies are always lower by about 3 eV and, secondly, the crossing point of the superoxide and the GS curves is reached now at a distance from the surface larger than the GS equilibrium distance. Both features are very important during the O_2 dissociation-enhancement process.

In order to provide more insight into this process, we first plot in Fig. 9 the DOS for the O_2 molecular orbitals intervening in the two bottom curves of Fig. 8 (oxygen in GS and O_2^-). Several remarks should be made from this figure. The GS oxygen DOS closely resembles both the DOS of the gas phase and the so-called physisorbed DOS in the adsorption of neutral O_2 on noble metals. However, the ground state of O_2 does *not* lead to the ground state of the adsorption system. The lowest curve at the estimated equilibrium distance (about 1.7–1.8 Å) corresponds instead to the configuration $O_2^- K^+ Si^*$. Its molecular DOS is given in the right panel of Fig. 9, showing the characteristic structure of the superoxide ion, with the following peaks: the doubly occupied π_x^* (at 0.3 and 1.3 eV), the singly occupied π_z^* (at 1.7 eV), and the doubly occupied π_y^* (at 4.2 and 5.1 eV), all measured with respect to the unperturbed Fermi level.

This structure agrees with the peroxy-bridge O_2^- , first seen by Hofer *et al.*³³ on Si(111), which constitutes the so-called precursor state that leads to dissociation. It is shown to be stable on this surface at liquid-nitrogen temperature and low coverage. Their near-edge x-ray-absorption fine-structure (NEXAFS) results prove, unam-

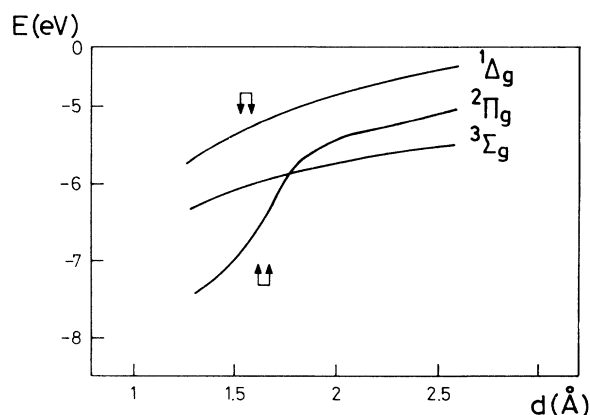


FIG. 8. Same as Fig. 4 but in the presence of the promoter.

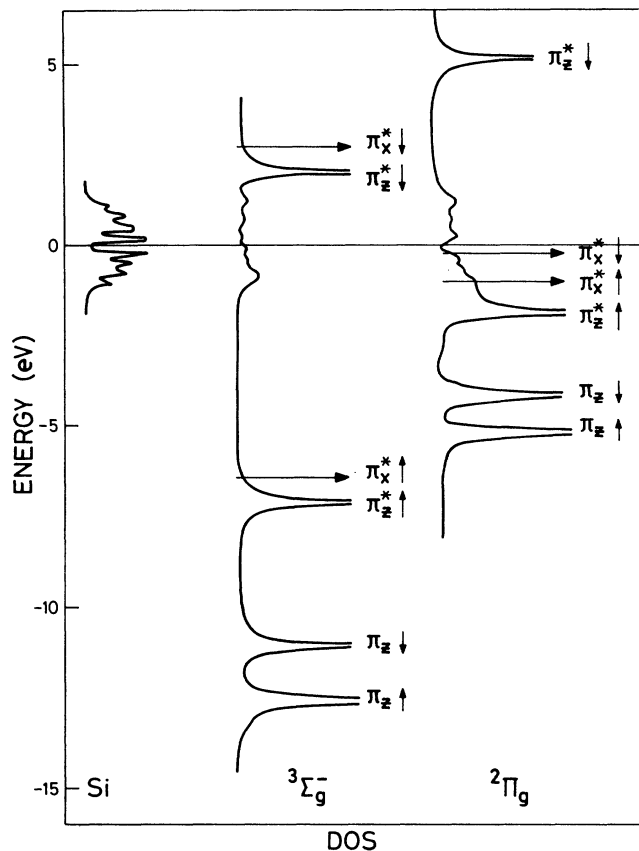


FIG. 9. Density of one-electron states for a Si atom in the vicinity of K^+ and for the oxygen molecule in both its ground state $^3\Sigma_g^-$ and the superoxide form $^2\Pi_g$ at their respective equilibrium distances. Energies are referred to the Fermi level.

biguously, its molecular character, with the molecular axis parallel to the surface and its O-O distance larger than in the O_2 isolated molecule. Their ultraviolet photoemission spectroscopy (UPS) results show two peaks at 2.1 and 3.9 eV, which these authors assign to the π_z^* and π_x^* molecular orbitals, respectively. Polarized UPS shows the π_z^* orbital to be normal to the surface. This oxygen state is also found to be stable on Si(100) covered with K, as reported by Michel *et al.*,³⁶ who observe an O-K-Si complex at any temperature. The complex obtained in the present work also agrees with this experimental result. At very low K coverage, the increase with temperature of the signal from these complexes reported by these authors could be due to an activated diffusion process of some of the species (O_2 and/or K) on the surface, rather than to a really active charge-transfer process.

Having described the result, we now discuss the mechanism of O_2^- formation in the presence of the promoter. The preadsorbed, partially ionized potassium atom influences the formation of superoxide in two main ways: (1) Its Coulomb interaction with the oxygen molecule leads to a further lowering of the affinity level of the latter by 0.5 eV. Without potassium, this affinity lowering was due only to the image potential of the neutral Si surface. (2) The s atomic orbital of potassium has a non-vanishing overlap with the π_x^* O_2 molecular orbital which entails an increase of the K-O hopping strength. This gives rise to a new alternative path to the formation of O_2^- different from the second-order spin-flip Helling transition. An important redistribution of energy levels and hence of charge takes place (compare Fig. 9, center and right panels) with a final formation of $O_2^-K^+Si^*$. Notice that this path would be blocked if potassium was adsorbed on other sites, like a bridge interrow position, since its overlap with π_x^* would then vanish.

IV. SUMMARIZING CONCLUSIONS

We have performed numerical calculations within the UHF formalism and have shown that (1) after adsorption of O_2 on clean Si(100), the formation of the O_2^- superoxide ion, precursor of the dissociated state, is an activated process. The rate-controlling step is excitation to the $^1\Delta_g$ O_2 state, as proposed by Helling, occurring via a second-order spin-flip process. (2) The adsorption of a single potassium atom on a valley-cave site leads to a charge transfer of about 0.9. This charge is essentially localized within the neighbor unit cells of silicon. It is in this region where the local action of preadsorbed K on O_2 dissociation takes place. In this process, the Hubbard term is very important. And, finally, (3) the local effect in the K-promoted O_2 dissociation is due to both the lowering of the O_2 affinity level by the local field of the partially ionized potassium atom and the opening of a new first-order reaction path, alternative to Helling excitation, for the formation of O_2^- with a considerable redistribution of charge leading to the formation of $O_2^-K^+Si$. In the language of BO curves, there is a curve crossing with the ionic $^2\Pi_g$ before reaching the minimum of the adiabatic $^3\Sigma_g^-$ curve.

ACKNOWLEDGMENT

Financial support of the Spanish Ministry of Education and Science through DGICYT Project No. PS90-0002 is acknowledged.

¹E. A. Lewis and E. A. Irene, *J. Vac. Sci. Technol. A* **4**, 916 (1986).

²A. Cros, J. Derrier, and F. Salvan, *Surf. Sci.* **110**, 471 (1981).

³A. D. Katnani, P. Pafetti, T. X. Zhao, and G. Margaritondo, *Appl. Phys. Lett.* **40**, 619 (1982).

⁴I. Abbati, G. Rossi, L. Callinarl, L. Braicovich, I. Lindau, and W. E. Spicer, *J. Vac. Sci. Technol.* **21**, 409 (1982).

⁵G. Rossi, L. Caliarì, I. Abbati, L. Braicovich, I. Lindau, and W. E. Spicer, *Surf. Sci.* **116**, L202 (1982).

⁶J. Derrier and F. Ringeisen, *Surf. Sci.* **124**, 235 (1983).

- ⁷A. Franciosi, S. Chang, P. Philip, C. Caprile, and J. Joyce, *J. Vac. Sci. Technol. A* **3**, 933 (1985).
- ⁸F. V. Hillebrecht, M. Ronay, D. Rieger, and F. J. Himpsel, *Phys. Rev. B* **34**, 5377 (1986).
- ⁹A. Franciosi, P. Soukiassian, P. Philip, S. Chang, A. Wall, A. Raisanen, and N. Troullier, *Phys. Rev. B* **35**, 910 (1987).
- ¹⁰E. M. Oellig and R. Miranda, *Surf. Sci. Lett.* **117**, 1947 (1986).
- ¹¹M. C. Asensio, E. G. Michel, E. M. Oellig, and R. Miranda, *Appl. Phys. Lett.* **51**, 1714 (1987).
- ¹²J. E. Ortega, E. M. Oellig, J. Ferrón, and R. Miranda, *Phys. Rev. B* **36**, 6213 (1987).
- ¹³H. I. Starnberg, P. Soukiassian, M. H. Bakshi, and Z. Hurych, *Phys. Rev. B* **37**, 1315 (1988).
- ¹⁴P. Soukiassian, T. M. Gentle, M. H. Bakshi, and Z. Hurych, *J. Appl. Phys.* **60**, 4339 (1986).
- ¹⁵P. Soukiassian, M. H. Bakshi, Z. Hurych, and T. M. Gentle, *Phys. Rev. B* **35**, 4176 (1987).
- ¹⁶P. Soukiassian, T. M. Gentle, M. H. Bakshi, A. S. Bommanavar, and Z. Hurych, *Phys. Scr.* **35**, 757 (1987).
- ¹⁷M. H. Bakshi, P. Soukiassian, T. M. Gentle, and Z. Hurych, *J. Vac. Sci. Technol. A* **5**, 1425 (1987).
- ¹⁸H. I. Starnberg, P. Soukiassian, and Z. Hurych, *Phys. Rev. B* **39**, 12 775 (1989).
- ¹⁹H. Ernst and M. L. Yu, *Phys. Rev. B* **41**, 12 953 (1990).
- ²⁰G. R. Castro, P. Pervant, E. G. Michel, R. Miranda, and K. Wandelt, *Vacuum* **41**, 787 (1990).
- ²¹J. K. Norskov, S. Holloway, and N. D. Lang, *Surf. Sci.* **137**, 65 (1984); N. D. Lang, S. Holloway, and J. K. Norskov, *ibid.* **150**, 24 (1985).
- ²²B. Hellsing, *Phys. Rev. B* **40**, 3855 (1989).
- ²³I. Panas and P. Siegbahn, *Chem. Phys. Lett.* **153**, 458 (1988); I. Panas, P. Siegbahn, and U. Wahlgren, *ibid.* **90**, 6791 (1989).
- ²⁴E. Artacho and F. Yndurain, *Phys. Rev. Lett.* **62**, 2491 (1989); *Phys. Rev. B* **42**, 11310 (1990).
- ²⁵J. M. López Sancho, M. C. Refolio, M. P. López Sancho, and J. Rubio, *Surf. Sci.* **285**, L491 (1993); *J. Vac. Sci. Technol. A* **11**, 2483 (1993).
- ²⁶E. G. Michel, P. Pervan, G. R. Castro, R. Miranda, and K. Wandelt, *Phys. Rev. B* **45**, 11 811 (1992).
- ²⁷R. A. Wolkow, *Phys. Rev. Lett.* **68**, 2636 (1992).
- ²⁸F. H. Stillinger, *Phys. Rev. B* **46**, 9590 (1992).
- ²⁹W. A. Harrison, *Electronic Structure and the Properties of Solids* (Freeman, San Francisco, 1980).
- ³⁰W. A. Goddard III, A. Redondo, and T. MacGill, *Solid State Commun.* **18**, 981 (1976).
- ³¹N. Mataga and K. Nishimoto, *Z. Phys. Chem.* **13**, 140 (1957).
- ³²D. E. Ramaker, *Phys. Rev. B* **21**, 4608 (1980).
- ³³U. Höfer, P. Morgen, W. Wurth, and E. Umbach, *Phys. Rev. Lett.* **55**, 2979 (1985); U. Höfer, P. Morgen, and W. Wurth, *Phys. Rev. B* **40**, 1130 (1989).
- ³⁴H. Sambe and D. E. Ramaker, *Surf. Sci.* **269/270**, 444 (1992).
- ³⁵T. Kendelewicz, P. Soukiassian, R. S. List, J. C. Woicik, P. P. Pianetta, I. Lindau, and W. E. Spicer, *Phys. Rev. B* **37**, 7115 (1988).
- ³⁶E. G. Michel, J. E. Ortega, E. M. Oellig, M. C. Asensio, J. Ferrón, and R. Miranda, *Phys. Rev. B* **38**, 13 399 (1988).
- ³⁷Ye Ling, A. J. Freeman, and B. Delley, *Phys. Rev. B* **39**, 10 144 (1989).